Performance of Retransmission Schemes for Multicasting in Random Wireless Networks

Mohammad G. Khoshkholgh*, Keivan Navaie‡, Kang G. Shin†, Victor C. M. Leung*

*The University of British Columbia (m.g.khoshkholgh@gmail.com, vleung@ece.ubc.ca)
‡Lancaster University (k.navaie@lancaster.ac.uk), †The University of Michigan (kgshin@umich.edu)

***Abstract*—We analyze retransmission schemes for multicast communications in random (ad hoc) wireless networks, where up to T retransmissions are utilized to reliably deliver each data packet to a set of destination receivers. To capture the effect of T on the network performance, we define *effective throughput* as a function of the multicast data rate, the percentage of receivers that have successfully decoded the multicast packet during T retransmissions, and T^{γ} (T to power γ). For a given scenario, $\gamma > 0$ indicates the corresponding performance requirements. For instance, when reliability is more important than the system capacity, γ is assigned a larger value, than scenarios in which higher energy-efficiency but moderate multicast coverage is required. We then investigate effective throughput under blunt retransmission (BR), chase combining (CC), and incremental redundancy (IR) schemes. To this aim, analytical tools from stochastic geometry and Poisson point processes are used. Our simulations confirm the accuracy of our analytical findings. The simulation results reveal interesting behaviors of retransmission schemes. For instance in a typical setting, the IR scheme is shown to improve the effective throughput by 200-400% (50-100%) over the BR scheme (CC scheme), without incurring additional signaling overhead.**

I. Introduction

There are numerous applications of multicast communication in random (ad hoc) wireless networks, such as machine-to-machine (M2M) and device-to-device (D2D) communications [1]. In such networks, gateways require to periodically multicast information to facilitate the formation of machine clusters in applications such as automation and smart grid. It is also used as a tool for efficient utilization of network resource, e.g., improving energy-efficiency in D2D through proximity-aware social networking and media sharing [2].

Multicasting in random networks is however very challenging due to excessive interference among multicast sessions resulting in high packet error rate. In contrast to the infrastructures-based systems, random networks commonly lack centralized protocols and entities, and hence distributed mechanisms are usually required for managing multicast communications and effectively dealing with high packet error rates. To be fully implementable in random networks, multicast mechanisms need to (*i*) demonstrate a certain level of robustness against lack or inaccuracy of the channel state information at the transmitters (CSIT), (*ii*) keep the signaling overhead at a manageable level, (*iii*) be able to guarantee successful delivery of multicast packets to all destination nodes, and (*iv*) be energy-efficient so as not to drain the device batteries. At the same time, as major efficiency metrics, multicast protocols need to provide an acceptable level of network transmission capacity and multicast delay. Nevertheless, many proposed multicast schemes and protocols are designed solely for, and tested against isolated scenarios such as a single multicast cluster. Ignoring the effects of interference amongst the multicast sessions in distributed networks result in inaccuracies and thus practical performance problems.

Our objective of this paper is to investigate the performance of multicasting schemes in random wireless networks; in particular, we focus on chase combining (CC), and incremental redundancy (IR) [6], [7], [10] schemes. As a benchmark for our performance analysis, we compare the performance of these two schemes against that of blunt retransmission (BR) [5]. To the best of our knowledge, this is the first performance analysis of CC and IR.

The BR scheme, also referred to as *repetitive transmission multicast*, retransmits packets multiple times within a permissible decoding interval, $T \geq 1$, time slots. BR is, in fact, an extension of the well-known automatic repeat request (ARQ) to the multicast paradigm (e.g., [6], [7]) and is shown in [5] to be an effective way to improve the network's transmission capacity defined as the accumulated network's throughput subject to the multicast outage constraint. In [8], we have extended the approach in [5] to analyze the associated delay performance of the BR scheme, showing its rather poor performance. The extended multicast delay also degrades energy-inefficiency which is of critical importance in many of M2M/D2D applications. To address this issue, the authors of [9] proposed a scheme based on occasional communication infrastructure assistance for efficient delivery of multicast packets. Although very effective in enhancing the multicast performance in D2D networks, such schemes impose extra signaling overheads on both the infrastructure and devices. The need for intervention by an infrastructure-based network might also not be achievable in many practical systems and scenarios such as ad hoc networks and disaster management systems. The CC and IR techniques are, on the other hand, entirely distributed and impose no extra signaling overheads, thus being suitable for multicasting in random networks.

To study the multicast performance, we introduce a new performance metric called *effective throughput* which is proportional to the multicast data rate multiplied by the percentage of receivers that can successfully decode the multicast packet during T retransmissions. The thus-defined effective throughput is also inversely proportional to T^γ, and $\gamma > 0$. We then show that by adjusting γ, one can balance various performance metric such as multicast delay and energy-efficiency. We adopt tools in stochastic geometry (e.g., [3], [4]) to evaluate the performance of CC and IR schemes, as they are shown to be capable of analyzing the performance aspects of multicasting in random networks [5]. Our analysis considers low-mobility random wireless networks as in [11], [12] which is shown capable of characterizing most of practical M2M systems. Thus, our analysis in this paper is different from that of [10] that focused on high-mobility scenarios in broadcasting networks.

We also study the accuracy of our analysis through simulations. Our simulation results show a significant performance improvement over the BR scheme even when the available number of retransmissions are as small as 5–10. For a typical setting, IR improves the effective throughput by 200-400 %, and CC by 50-100 % over BR.

II. Multicast Networks

The source nodes X_i in our multicast communication model share the same radio spectrum. In this model, the source nodes belong to a Poisson Point Process (PPP) set, Φ, with density λ. Each X_i transmits packets to a set of destination/receiver nodes in its coverage area which is referred to as *cluster* i. We define a disk $\mathcal{R}_i$ of radius $s > 1$ associated with X_i. Destination nodes are randomly placed in each cluster i according to homogeneous marked PPP, Φ_i^r, with intensity measure λ_r. For any two clusters i and i', Φ_i^r and $\Phi_{i'}^r$ are independent. This model allows clusters to overlap, and thus some clusters may contain other active sources and unintended destination nodes. In this model, spatial distribution of the source nodes forms a homogeneous marked PPP, Φ, with spatial density λ.

The network is then modeled with set $\mathcal{Z} = \bigcup_{X_i \in \Phi} (\Phi_i^r \cup X_i)$, which is a Poisson Cluster Process (PCP) with density $\Xi = \pi s^2 \lambda_r \lambda$, where Ξ is the average number of destination nodes in each cluster. Stationarity makes it sufficient to measure the network performance in a typical cluster, $\mathcal{R}_0$, associated with a source node X_0 located at the origin.

Set $\Phi_0^r = \{(Y_j, H_j), Y_j \in \mathcal{R}_0, H_j \geq 0, j \in \mathbb{N}_+\}$ is a collection of 2-tuples each including destination node, Y_j, and a corresponding fading mark, H_j, that represents the wireless channel power gain between X_0 and Y_j. Fading is location-independent with a unit-mean exponential probability density function (pdf). Transmitters/sources in $\Phi = \{(X_i, \tilde{H}_{ij}), X_i \in \mathbb{R}^2, \tilde{H}_{ij} \geq 0, i \in \mathbb{N}_+, j \in \mathbb{N}_+\}$ are drawn from the same pdf unit-mean exponential fading, where $\tilde{H}_{ij}$ is the interfering channel power gain between transmitter i and receiver j at the cluster $\mathcal{R}_0$ $\tilde{H}_{ij}$, and independent of H_j.

The quality of link $j \in \Phi_0^r$ is determined by Signal-to-Interference Ratio (SIR) defined as

$$\mathrm{SIR}_j[t] = \frac{\|Y_j\|^{-\alpha} H_j[t]}{\sum\limits_{i \in \Phi / X_0} \|X_i - Y_j\|^{-\alpha} \tilde{H}_{ij}[t]}, \tag{1}$$

where t represents time slot. In (1), $\|Y_j\|$ is the Euclidian distance between transmitter X_0 and receiver X_j, $\alpha > 2$ is the path-loss exponent, and $\|Y_j\|^{-\alpha}$ is the distance-dependent path-loss attenuation. For brevity, we assume that all source nodes use the same transmit power. An outage will occur if $\mathrm{SIR}_j < \beta$, where β is the receiver SIR threshold. In this setting, an outage incident is equivalent to unsuccessful decoding of a multicast packet. By following the same line of argument as in [5] and [9], one can show that it suffices to focus on the statistics of the aggregated interference measured at the origin, I_0, for the purpose of studying the system performance.

In this model, time is slotted and packets must be successfully decoded by all the receiver nodes in each cluster, so each multicast packet may be required to be retransmitted up to T times. This (T) parameter also represents the permissible decoding delay. Note that in our setting, the fading coefficients change randomly from one time slot to another. Furthermore, in case of low mobility, the positions of both transmitter and receiver nodes remain unchanged during the decoding interval, T, see, e.g., [11].

Let δ_j be a random variable associated to receiver node Y_j:

$$\delta_j = \sum_{t=1}^{T} 1\left\{\mathrm{SIR}_j[t] \geq \beta\right\}, \tag{2}$$

where $1\{x\} = 1$ if x is true and 0 otherwise. Eq. (2) indicates the number of times a multicast packet is successfully decoded at Y_j. If $\delta_j = 0$, receiver j is unable to decode the packet after T retransmissions, and thus experiences a multicast outage. Specifically, we are interested in the average number of receiver nodes, Ξ_{cov}, that will not experience multicast outages, where

$$\Xi_{\mathrm{cov}} = \mathbb{E} \sum_{j \in \Phi_0^r} 1(\delta_j > 0). \tag{3}$$

It is thus desirable to have Ξ_{cov} as close to Ξ as possible, where Ξ is the average number of receiver nodes in a cluster.

It is shown in [5], [8] that by increasing T, $\Xi_{\mathrm{cov}} \to \Xi$. The costs for this, however, are a large decoding delay, low effective transmission rate, and low energy-efficiency — these performance metrics are in fact interrelated and often conflict with each other. Different multicast schemes also behave differently in different scenarios.

A. Effective Throughput

To incorporate the number of retransmissions in the performance analysis and manage the impact of different realistic scenarios on the above mentioned trade-offs, we introduce *effective throughput* (ET) as a performance metric:

$$\eta_\gamma = \frac{\log(1+\beta)}{T^\gamma} \frac{\Xi_{\mathrm{cov}}}{\Xi}. \tag{4}$$

As shown in (4), by changing $\gamma > 0$, one may manipulate the effect of number of retransmission attempts, T, on the multicast communication performance so that levels of trade-offs among various performance metrics (according to the underlying network application) be preserved. For instance, if energy-efficiency has a high-priority design requirement, a high γ value will be considered. A small γ value, on the other hand, encourages a larger number of retransmissions, which might be necessary when delivering packets to receiver nodes has a higher priority than the network capacity, e.g., disaster management systems.

III. Performance Analysis

In this section we investigate the ET performance of three well-known retransmission schemes in wireless networks: (*i*) blunt retransmission (BR), (*ii*) chase-combining (CR), and (*iii*) incremental-redundancy (IR).

A. Blunt Retransmission

In the BR scheme, the source node retransmits the multicast packet up to T times. In each time slot t, the receiver nodes focus solely on decoding of the latest copy of the received packet, and discard the old copies [5], [6], [9]. The following proposition provides the ET of the BR scheme.

Proposition 1: ET of the BR scheme is

$$\eta_{\gamma}^{\mathrm{BR}} = \frac{\log(1+\beta)}{s^2 T^{\gamma}} \sum_{t=1}^{T} (-1)^{t+1} \binom{T}{t} \frac{1 - e^{-C(\alpha)\lambda t^{\check{\alpha}} \beta^{\check{\alpha}} s^2}}{C(\alpha)\lambda t^{\check{\alpha}} \beta^{\check{\alpha}}}, \tag{5}$$

where $C(\alpha) = \pi\Gamma(1+\check{\alpha})\Gamma(1-\check{\alpha})$ and $\check{\alpha} = 2/\alpha$.

Proof: Applying Campbell's Theorem [3] to (3), we get

$$\Xi_{\mathrm{cov}} = 2\pi\lambda_r \int_0^s \mathbb{P}\left\{\delta_y > 0\right\} y dy. \tag{6}$$

We also note that

$$\begin{aligned}\mathbb{P}\{\delta_y > 0\} &= \mathbb{E}_{\Phi}\mathbb{P}\left\{\sum_{t=1}^{T} \mathbf{1}\left(\mathrm{SIR}_y[t] \geq \beta\right) > 0 | \Phi\right\} \\ &= \sum_{t=1}^{T} (-1)^{t+1} \binom{T}{t} \mathbb{E}_{\Phi}\left(\mathbb{P}\left\{\mathrm{SIR}_y \geq \beta | \Phi\right\}\right)^t, \end{aligned} \tag{7}$$

where that last equation is due to [13] and independence of fading fluctuations across time slots. Note that our focus is on low-mobility scenarios, and thus conditioned on the position of interferers, the event $\mathrm{SIR}_y \geq \beta$ is independent and identical across time slots. Since fading is assumed to be Rayleigh, it is straightforward to show that

$$\begin{aligned}\mathbb{E}_{\Phi}\left(\mathbb{P}\left\{\mathrm{SIR}_y \geq \beta | \Phi\right\}\right)^t &= \mathbb{E}_{\Phi} e^{-t\beta y^{\alpha} \sum\limits_{X_i \in \Phi / X_0} \frac{\tilde{H}_i}{\|X_i\|^{\alpha}}} \\ &= e^{-C(\alpha)\lambda t^{\check{\alpha}} \beta^{\check{\alpha}} y^2}. \end{aligned} \tag{8}$$

Combining (8), (7), and (6), we obtain

$$\Xi_{\mathrm{cov}} = \pi\lambda_r \sum_{t=1}^{T} (-1)^{t+1} \binom{T}{t} \frac{1 - e^{-C(\alpha)\lambda t^{\check{\alpha}} \beta^{\check{\alpha}} s^2}}{C(\alpha)\lambda t^{\check{\alpha}} \beta^{\check{\alpha}}}. \tag{9}$$

Substituting (9) into (4) leads to (17) and completes the proof. □

B. Incremental Redundancy

The IR scheme is based on the concept of code combining, where the transmitter adds parity redundancy to the packet in each time slot t. Receiver node j then applies a code combining technique to decode the packet by jointly decoding the information as well as parity information received until t. The achievable data rate of destination node j is shown to be $\sum_{t=1}^{T} \log(1 + \mathrm{SIR}_j[t])$ [7]. Therefore, for node j

$$\delta_j^{\mathrm{IR}} = 1\left(\sum_{t=1}^{T} \log(1 + \mathrm{SIR}_j[t]) \geq \log(1+\beta)\right). \tag{10}$$

Therefore, the average number of receivers within the coverage is

$$\Xi_{\mathrm{cov}}^{\mathrm{IR}} = \mathbb{E} \sum_{j \in \Phi_0^r} 1(\delta_j^{\mathrm{IR}} > 0). \tag{11}$$

The energy efficency of IR is then obtained as

$$\eta_{\gamma}^{\mathrm{IR}} = \frac{\log(1+\beta)}{T^{\gamma}} \frac{\Xi_{\mathrm{cov}}^{\mathrm{IR}}}{\Xi}. \tag{12}$$

Evaluating (12) is a challenging task due mainly to the difficulty of evaluating multicast coverage probability, $\mathbb{P}\{\sum_{t=1}^{T} \log(1 + \mathrm{SIR}_j[t]) \geq \log(1+\beta)\}$. In the following proposition we provide an upper bound on the ET of the IR technique.

Proposition 2: An upper bound on the ET of the IR scheme with T allowable retransmission attempts is

$$\eta_{\gamma}^{\mathrm{IR}} \geq \frac{\log(1+\beta)}{s^2 T^{\gamma}} \frac{1 - e^{-\tilde{C}(\alpha) s^2 \Delta}}{\tilde{C}(\alpha)\lambda\Delta}, \tag{13}$$

where

$$\Delta = \int_0^{\infty} \dots \int_0^{\infty} e^{-\sum\limits_{t=1}^{T} h_t} \times \\ \left(\sum_{t=1}^{T} \left((1+\beta)^{\frac{1}{T}} \prod_{t' \neq t} h_{t'}^{\frac{1}{T}} - h_t\right) 1_{\{\prod\limits_{t' \neq t} \frac{h_{t'}}{h_t} > \frac{1}{1+\beta}\}}\right)^{\check{\alpha}} \prod_{t=1}^{T} dh_t. \tag{14}$$

Proof: See the Appendix. □

C. Chase-Combining Retransmission

The CC scheme is a time-diversity technique in which the receiver nodes softly combine T copies of the multicast packet by applying maximum ration combining (MRC) in time, e.g., [6], [7], [10]. Assuming T retransmission attempts, by following the same lines of argument as in [10], it is straightforward to show that the SIR for decoding the packet at destination node j is

$$\mathrm{SINR}_j^{\mathrm{CC}}[T] = \frac{\|Y_j\|^{-\alpha} \|\boldsymbol{h}_j[T]\|^2}{\sum\limits_{i \in \Phi / X_0} \|X_i - Y_j\|^{-\alpha} \tilde{H}_{ij}[T]}, \tag{15}$$

where $\|\boldsymbol{h}_j[T]\|^2$ is a Chi-squared random variable with $2T$ degrees-of-freedom (DoF), and $\tilde{H}_{ij}[T]$s are independent and identically distributed (i.i.d.) exponential random variables independent of $\|\boldsymbol{h}_j[T]\|^2$. The j-th receiver is in multicast outage, if $\delta_j^{\mathrm{CC}} = 1\left(\mathrm{SIR}_j[T] \geq \beta\right)$. Therefore, the average number of receivers in coverage is

$$\Xi_{\mathrm{cov}}^{\mathrm{CC}} = \mathbb{E} \sum_{j \in \Phi_0^r} 1(\delta_j^{\mathrm{CC}} > 0). \tag{16}$$

The following proposition provides the ET of the CC scheme.

Proposition 3: With the CC scheme and T retransmission attempts, ET is

$$\eta_\gamma^{\mathrm{CC}} = \frac{\log(1+\beta)}{s^2 T^\gamma} \sum_{t=0}^{T-1} \frac{(-1)^t}{t!} \frac{d^t}{dw^t} \frac{1 - e^{-w^{\tilde{\alpha}} \beta^{\tilde{\alpha}} s^2 C(\alpha) \lambda}}{w^{\tilde{\alpha}} \beta^{\tilde{\alpha}} C(\alpha) \lambda} \Big|_{w=1}. \tag{17}$$

Proof: To obtain $\Xi_{\mathrm{cov}}^{\mathrm{CC}}$ in , we the multicast coverage of a typical receiver node which is

$$\mathbb{P}\{\delta_y^{\mathrm{CC}} > 0\} = \mathbb{E}_\Phi \mathbb{P}\left\{\mathrm{SINR}_y^{\mathrm{CC}} \geq \beta | \Phi\right\}. \tag{18}$$

By noticing (15), (18) is then extended as

$$\begin{aligned}
\mathbb{P}\{\delta_y^{\mathrm{CC}} > 0\} &= \mathbb{E}_\Phi \mathbb{P}\left\{ \frac{y^{-\alpha}\|\boldsymbol{h}[T]\|^2}{\sum\limits_{i \in \Phi/X_0} \|X_i\|^{-\alpha} \tilde{H}_i[T]} \geq \beta | \Phi \right\} \\
&= \mathbb{E}_\Phi \int_0^\infty \mathcal{L}^{-1}_{\bar{\mathrm{F}}_{\|\boldsymbol{h}[T]\|^2}}(w) e^{-s\beta y^\alpha \sum\limits_{X_i \in \Phi/X_0} \frac{\tilde{H}_i}{\|X_i\|^\alpha}} dw \\
&= \int_0^\infty \mathcal{L}_{\bar{\mathrm{F}}^{-1}_{\|\boldsymbol{h}[T]\|^2}}(w) \mathbb{E}_\Phi \prod_{X_i \in \Phi/X_0} \mathbb{E}_{\tilde{H}_i} e^{-w\beta y^\alpha \frac{\tilde{H}_i}{\|X_i\|^\alpha}} dw \\
&= \int_0^\infty \mathcal{L}^{-1}_{\bar{\mathrm{F}}_{\|\boldsymbol{h}[T]\|^2}}(w) e^{-w^{\tilde{\alpha}} \beta^{\tilde{\alpha}} y^2 C(\alpha)\lambda} dw,
\end{aligned} \tag{19}$$

where $\mathcal{L}_{\bar{\mathrm{F}}^{-1}_{\|\boldsymbol{h}[T]\|^2}}(w)$ is the inverse Laplace transform of $\bar{\mathrm{F}}_{\|\boldsymbol{h}[T]\|^2}$ and is equal to $\sum\limits_{t=0}^{T-1} \frac{1}{t!}\delta^{(t)}(w-1)$, and $\delta^{(t)}(w)$ is the t-th derivative of Dirac delta function [10]. Utilizing (19), we then write

$$\begin{aligned}
&\int_0^s \int_0^\infty \mathcal{L}^{-1}_{\bar{\mathrm{F}}_{\|\boldsymbol{h}[T]\|^2}}(w) e^{-w^{\tilde{\alpha}} \beta^{\tilde{\alpha}} y^2 C(\alpha)\lambda} dwydy \\
&= \int_0^\infty \mathcal{L}^{-1}_{\bar{\mathrm{F}}_{\|\boldsymbol{h}[T]\|^2}}(w) \int_0^s e^{-w^{\tilde{\alpha}} \beta^{\tilde{\alpha}} y^2 C(\alpha)\lambda} ydydw \\
&= \int_0^\infty \sum_{t=0}^{T-1} \frac{1}{t!}\delta^{(t)}(w-1) \int_0^s e^{-w^{\tilde{\alpha}} \beta^{\tilde{\alpha}} y^2 C(\alpha)\lambda} ydydw \\
&= \sum_{t=0}^{T-1} \frac{(-1)^t}{t!} \frac{d^t}{dw^t} \frac{1 - e^{-w^{\tilde{\alpha}} \beta^{\tilde{\alpha}} s^2 C(\alpha)\lambda}}{w^{\tilde{\alpha}} \beta^{\tilde{\alpha}} C(\alpha)\lambda} \Big|_{w=1}.
\end{aligned} \tag{20}$$

Substituting (20) in (4) completes the proof. □

D. Simulation Results

We now investigate the accuracy of our analytical results. We further compare the performance of BR, CC, and IR schemes. The Monte Carlo simulation method is adopted with large enough snapshots. In each snapshot, we randomly distribute transmitters within a disk of radius 5000 units. Receivers associated with each transmitter are distributed in the multicast clusters. We also set $\lambda_t = 0.01$, $\lambda_r = 0.02$, $s = 10$ units, $\beta = 20$, and $\alpha = 4$.

Fig. 1, 2, and 3 show comparisons between our analysis and simulation results for different γ values. Each figure provides ET *vs.* T, the number of retransmission attempts. For both cases of BR and CC, the simulation results are shown to closely follow the analysis. For the IR scheme, Proposition 2 provides also a reasonably accurate upper bound that follows the trends observed in the simulation results. The IR scheme, and the analysis results are are shown to be more accurate for smaller γ values, i.e., when delay is not a main concern.

By comparing the results in Figs. 1–3, we also find that BR, CC, and IR schemes behave differently in response to the changes in T for different γ values. For example, Fig. 1 indicates that increasing T is in general beneficial for small γ values, i.e., when delay is not a main concern. Nevertheless, the IR's ET is shown to increase substantially while the ET improvement for CC is rather moderate. Increasing T, however, does not result in a significant change of the BR's ET. This figure also shows that for $T = 10$ retransmission attempts, the IR (CC) scheme achieves almost 400 $\%$ (100$\%$) higher ET than the BR scheme. Note that for $T > 10$, increasing T in the IR scheme does not improve ET, thus becoming not beneficial.

For $\gamma = 0.75$, however, Fig. 2 shows that increasing T is not necessarily beneficial even in the IR scheme. In fact, the best performance in this case is achieved when $T = 5$. For this number of retransmissions, a 200% improvement in the ET performance is seen over the BR scheme. Any further increase of T causes reduction of ET for both CC and BR schemes, but the CC scheme still demonstrates 50% higher ET than the BR scheme. Finally, for $\gamma = 1$, Fig. 3 shows that increasing T results in a significant reduction of ET for both BR and and CC schemes. In fact, 10x growth of T causes about 100 $\%$ reduction of ET in the BR scheme. In contrast, increasing T is shown to be beneficial in the IR scheme. The best performance is achieved for the BR scheme when $T = 4$. For this number of retransmission attempts IR makes a 150% ET enhancement over BR.

Comparing the results in these figures, we conclude that the IR scheme outperforms the CC and BR schemes. Also, by increasing γ, the number of retransmission attempts that reduces the maximum ET as well as the ET gain compared to the BR scheme.

IV. Conclusions

We studied the performance of multicast retransmission schemes including bunt retransmission (BR), chase combining (CC), and incremental redundancy (IR) in random wireless

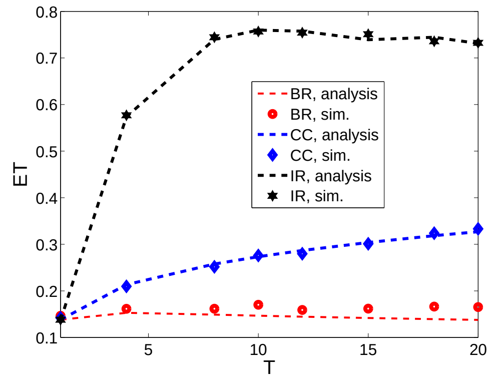

Fig. 1. ET of the BR, CC and IR schemes *vs.* the number of retransmissions, T, for $\gamma = 0.25$.

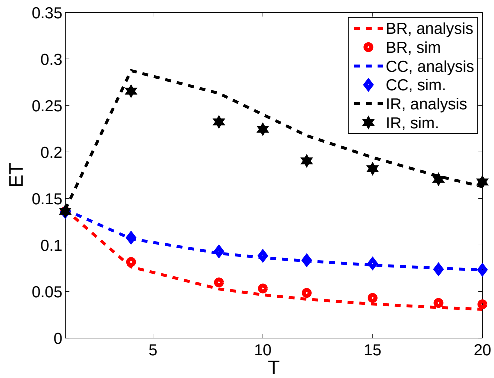

Fig. 2. ET of the BR, CC and IR schemes *vs.* number of retransmissions, T, for $\gamma = 0.75$.

networks. We introduced effective throughput (ET) as a performance metric to represent the performance requirements in a given multicasting scenario, and also evaluated ET for the above retransmission schemes using analytical tools in stochastic geometry. Our simulations confirmed the accuracy of our analysis. The simulation results have also shown substantial benefits of IR and CC schemes in improving multicast performance. We have further observed that up to $150-400\%$ performance enhancement is achieved with the IR scheme when T is carefully selected.

References

[1] J.-M. Vella and S. Zammit, "A survey of multicasting over wireless access networks," *IEEE Communications Surveys & Tutorials*, vol. 15, no. 2, pp. 718–753, Second Quarter 2013.

[2] A. Asadi *et al.*, "A survey on device-to-device communication in cellular networks," *IEEE Communications Surveys & Tutorials*, vol. 16, no. 4, pp. 1801–1819, 4th Quarter 2014.

[3] M. Haenggi and R. K. Ganti, "Interference in large wireless networks," *Foundations and Trends in Networking*, vol. 3, no. 2, 2008, Available at http://www.nd.edu/ mhaenggi/pubs/now.pdf.

[4] M. Haenggi, J. G. Andrews, F. Baccelli, O. Dousse, and M. Franceschetti, "Stochastic geometry and random graphs for the analysis and design of wireless networks," *IEEE Journal on Selected Areas in Communications*, vol. 27, no. 7, pp. 1029–1046, September 2009.

[5] C.-H. Liu and J. G. Andrews, "Multicast outage probability and transmission capacity of multihop wireless networks," *IEEE Transactions on Information Theory*, vol. 57, no. 7, pp. 4344–4358, July 2011.

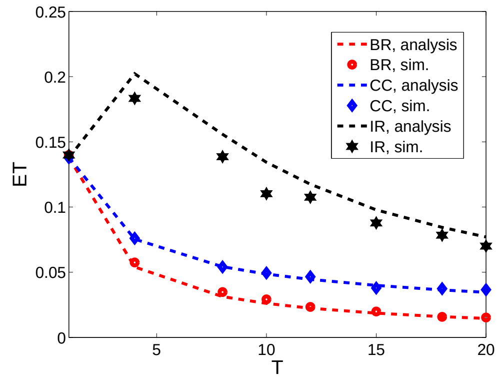

Fig. 3. ET of the BR, CC and IR schemes *vs.* number of retransmissions, T, for $\gamma = 1$.

[6] M. Afshang *et al.*, "Coverage and area spectral efficiency of clustered device-to-device networks," *in Proc. IEEE GLOBECOM*, Dec. 2015.

[7] G. Caire and D. Tuninetti, "The throughput of hybrid-ARQ protocols for the gaussian collision channel," *IEEE Trans. Information Theory*, vol. 47, no. 5, pp. 1971–1988, Jul. 2001.

[8] M. G. Khoshkholgh *et al.*, "On the impact of delay constraint on the multicast outage in wireless fading environment," *IEEE ICC*, pp. 3714–3719, 2015.

[9] X. Lin *et al.*, "Modeling, analysis, and optimization of multicast device-to-device transmisisons," *IEEE Trans. Wireless Comm.*, vol. 13, no. 8, pp. 4346–4359, Aug. 2014.

[10] W. C. Ao *et al.*, "Bounds and exact mean node degree and node isolation probability in interference-limited wireless ad hoc networks with general fading," *IEEE TVT*, vol. 61, no. 5, pp. 2342–2348, Jun. 2012.

[11] F. Baccelli *et al.*, "A new phase transition for local delays in MANETs," *IEEE IFOCOM*, 2010.

[12] M. Haenggi, "The local delay in poisson networks," *IEEE Trans. Inf. Theory*, vol. 59, pp. 1788–1802, Mar. 2013.

[13] M. Haenggi and R. Smarandache, "Diversity polynomials for the analysis of temporal correlations in wireless networks," *IEEE Trans. on Wireless Comm.*, vol. 12, no. 11, pp. 5940–5951, Nov. 2013.

Appendix: Proof of Proposition 2

According to (10), the coverage probability associated with receiver node j is

$$\mathbb{P}\{\delta_j^{\mathrm{IR}} > 0\} = \mathbb{P}\left\{\sum_{t=1}^{T} \log(1+\mathrm{SINR}_j[t]) \geq \log(1+\beta)\right\}. \tag{21}$$

To obtain the coverage probability in (21), we need to evaluate the distributed function of random variable, $\sum_{t=1}^{T} \log(1+\mathrm{SINR}_j[t])$, which is very complicated and unknown to the related literature. To address this issue, we introduce an auxiliary parameters $R_t \geq 0$, where $\log(1+\beta) = \sum_t R_t$, i.e., the required transmitted data rate, $\log(1+\beta)$, is split across T time slots, each with rate R_t. For now, assuming that R_ts are known, the coverage probability (21) is reduced to

$$\begin{aligned}
\mathbb{P}\{\delta_j^{\mathrm{IR}} > 0\} &= \mathbb{E}_\Phi \mathbb{P}\left\{\mathrm{SINR}_j[t] \geq e^{R_t} - 1, \forall t | \Phi\right\} \\
&= \mathbb{E}_\Phi \prod_{t=1}^{T} \mathbb{P}\left\{\mathrm{SINR}_j[t] \geq e^{R_t} - 1 | \Phi\right\} \\
&= \mathbb{E}_\Phi \prod_{t=1}^{T} \mathbb{E}_{\tilde{H}_i[t]} e^{-(e^{R_t}-1)y^\alpha \sum\limits_{X_i \in \Phi/X_0} \frac{\tilde{H}_i[t]}{\|X_i\|^\alpha}}
\end{aligned}$$

$$= \mathbb{E}_{\Phi} \prod_{X_i \in \Phi / X_0} \mathbb{E}_{\{\tilde{H}_i[t]\}_t} e^{-y^{\alpha} \frac{\sum_{t=1}^{T} (e^{R_t}-1)\tilde{H}_i[t]}{\|X_i\|^{\alpha}}}$$

$$= e^{-\tilde{C}(\alpha) y^2 \lambda \Delta}, \tag{22}$$

where the last step is obtained using the Laplace transform of the shot noise processes (see [4]) and Δ is

$$\Delta = \mathbb{E}\left[(\sum_{t=1}^{T} (e^{R_t} - 1)\tilde{H}[t])^{\check{\alpha}} \right]. \tag{23}$$

Using (22) the average number of receivers in the coverage is

$$\Xi_{\text{cov}} = 2\pi\lambda_r \int_0^s e^{-\tilde{C}(\alpha) y^2 \lambda \Delta} y dy.$$

$$= \pi\lambda_r \frac{1 - e^{-\tilde{C}(\alpha) s^2 \lambda \mathbb{E}\left[(\sum_{t=1}^{T} (e^{R_t}-1)\tilde{H}[t])^{\check{\alpha}} \right]}}{\tilde{C}(\alpha)\lambda\Delta}.$$

Consequently,

$$\frac{\Xi_{\text{out}}}{\Xi} = \frac{1}{s^2} \frac{1 - e^{-\tilde{C}(\alpha) s^2 \lambda \Delta}}{\tilde{C}(\alpha)\lambda\Delta} \tag{24}$$

$$= \sum_{n=1}^{\infty} \frac{(-1)^{n+1} (\tilde{C}(\alpha) s^2 \lambda)^n}{n!} \Delta^n, \tag{25}$$

where in the last step we have simply substituted the series representation of the exponential function. Now, let's derive the values for R_t so that (25) is maximized as follows.

$$\max \sum_{n=1}^{\infty} \frac{(-1)^{n+1} (\tilde{C}(\alpha) s^2 \lambda)^n}{n!} \Delta^n$$

$$s.t. \quad \sum_t R_t = \log(1+\beta). \tag{26}$$

This results in an upper bound of the corresponding ET performance.

Introducing Lagrange multiplier $\mu \geq 0$, the Lagrange problem associated with the optimization problem (26) is

$$L = \max_{R_t \geq 0} \sum_{n=1}^{\infty} \frac{(-1)^{n+1} (\tilde{C}(\alpha) s^2 \lambda)^n}{n!} \Delta^n - \mu \sum_t R_t.$$

By taking derivatives of L with respect to $R_{t'}$ $\forall t'$, and setting the result to zero, we obtain

$$\mu = \sum_{n=1}^{\infty} \frac{(-1)^{n+1} (\tilde{C}(\alpha) s^2 \lambda)^n}{(n-1)!} (\mathbb{E}(\sum_{t=1}^{T} (e^{R_t} - 1)\tilde{H}[t])^{\check{\alpha}})^{n-1}$$

$$\int_0^{\infty} \dots \int_0^{\infty} \check{\alpha} (\sum_{t=1}^{T} (e^{R_t} - 1) h_t)^{\check{\alpha}-1} h_{t'} e^{R_{t'}} \prod_{t=1}^{T} \mathrm{f}_{\tilde{H}[t]}(h_t) dh_t$$

$$\forall t' = 1, \dots, T.$$

Therefore, $\forall t' \neq t$

$$\int_0^{\infty} \dots \int_0^{\infty} \frac{h_{t'} e^{R_{t'}} - h_{t''} e^{R_{t''}}}{(\sum_{t=1}^{T} (e^{R_t} - 1) h_t)^{-\check{\alpha}+1}} \prod_{t=1}^{T} \mathrm{f}_{\tilde{H}[t]}(h_t) dh_t = 0,$$

or equivalently,

$$h_t e^{R_t} = h_{t'} e^{R_{t'}}, \ t' \neq t. \tag{27}$$

Solving (27) for R_t, we obtain

$$R_t = R_{t'} + \log \frac{h_{t'}}{h_t}, \ t' \neq t. \tag{28}$$

Summation of both sides in (28) $\forall t' \neq t''$ yields:

$$(T-1) R_t = \sum_{t' \neq t} R_{t'} + \log \left(\prod_{t' \neq t} \frac{h_{t'}}{h_t} \right). \tag{29}$$

Recalling that $\sum_t R_t = \log(1+\beta)$, (29) is simplified to

$$R_t = T^{-1} \log(1+\beta) + T^{-1} \log \left(\prod_{t' \neq t} \frac{h_{t'}}{h_t} \right). \tag{30}$$

Using (30) and noting $R_t \geq 0$, (23) is

$$\Delta = \mathbb{E} \left(\sum_{t:\, \prod_{t' \neq t} \frac{\tilde{H}[t']}{\tilde{H}[t]} > \frac{1}{1+\beta}} (1+\beta)^{\frac{1}{T}} \prod_{t' \neq t} \tilde{H}^{\frac{1}{T}}[t'] - \tilde{H}[t] \right)^{\check{\alpha}}. \tag{31}$$

Assuming an independent exponential distribution for interfering channels, (31) is further extended to

$$\Delta = \int_0^{\infty} \dots \int_0^{\infty} e^{-\sum_{t=1}^{T} h_t} \prod_{t=1}^{T} dh_t \times$$

$$\left(\sum_{t=1}^{T} \left((1+\beta)^{\frac{1}{T}} \prod_{t' \neq t} h_{t'}^{\frac{1}{T}} - h_t \right) 1_{\{\prod_{t' \neq t} \frac{h_{t'}}{h_t} > \frac{1}{1+\beta}\}} \right)^{\check{\alpha}}. \tag{32}$$

Substituting (32) into (24) completes the proof.